



Agricultural intensification during the Late Holocene rather than climatic aridification drives the population dynamics and the current conservation status of *Microtus cabreræ*, an endangered Mediterranean rodent

José Antonio Garrido-García^{1,2*}  | Diego Nieto-Lugilde^{3,4*}  | Francisca Alba-Sánchez⁴  | Ramón C. Soriguer¹ 

¹Estación Biológica de Doñana (CSIC), Sevilla, Spain

²Instituto Geológico y Minero de España (IGME), Madrid, Spain

³Appalachian Laboratory, University of Maryland Center for Environmental Science, Frostburg, MD, USA

⁴Departamento de Botánica, Universidad de Granada, Granada, Spain

Correspondence

José Antonio Garrido-García, Instituto Geológico y Minero de España (IGME), Madrid, Spain.
Email: ja.garrido@igme.es

Funding information

Spanish Ministry of Economy and Competitiveness; Andalusian Regional Government; Andalusian Government Environment Department

Editor: Jenny McGuire

Abstract

Aim: Disentangling the relative importance of climatic and anthropogenic factors is crucial in conservation biology but problematic using short-term data only. Long-term (palaeobiological) data are thus increasingly being used to understand taxon history and to identify potential status and baseline (pre-anthropogenic) conditions, which in turn allows the optimization of species conservation plans. We combined species distribution models (SDMs) with current and palaeo-occurrences of *Microtus cabreræ*, a threatened Mediterranean rodent, to circumvent the limitations of the palaeorecord (e.g. spatio-temporal bias), to characterize this rodent's history (potential status and baseline conditions) since the Mid-Holocene (~6,000 yr BP), and to determine the relative importance of climatic and anthropogenic factors in its decline.

Location: Historic distributional range of *M. cabreræ* (Iberian Peninsula and SE France).

Methods: We used generalized linear models (GLMs) to study the effects of four climatic (temperature and precipitation seasonality, minimum temperature, aridity) and four anthropogenic variables (human influence index, surface area of irrigated crops, rain-fed crops and pastures) on the species' current distribution. Then, we used an ensemble of SDMs to estimate its current and Mid-Holocene potential distributions based only on climate variables, and validated model projections against current and palaeo records. Finally, suitability maps were analysed to study the species' range dynamics during the Late Holocene.

Results: *Microtus cabreræ*'s current distribution is constrained by both climatic and anthropogenic variables. Temperature and precipitation seasonality—but not aridity or minimum temperature—play an important positive role in constraining its distribution, but agriculture is the main human activity that affects it negatively. Climatic changes during the Late Holocene probably led to an expansion of its distribution without fragmentating its range.

*These authors contributed equally to this work.

Main conclusions: Contrary to previous hypotheses, under natural conditions, *M. cabreræ* should be in an expansive phase of its taxon cycle. Yet, its potential and current conservation status is negatively affected by agricultural habitat destruction, suggesting that conservation strategies should aim to control agricultural intensification.

KEYWORDS

agriculture intensification, aridification, ensemble modelling, fossil record, Iberian Peninsula, land use change, Late Holocene, *Microtus cabreræ*, species distribution models

1 | INTRODUCTION

Climate and anthropogenic pressures are important drivers that shape biodiversity patterns and species distributions (Lorenzen et al., 2011) and so are potential threat factors (Lima-Ribeiro, Nogués-Bravo, Terribile, Batra, & Diniz-Filho, 2013), contributing to the current conservation status of threatened species. However, their implications for conservation are quite different: although anthropogenic threats can be counterbalanced by laws or conservation measures, mitigation of climatic threats is a far more complex process, limited to intensive and economically expensive actions with unpredictable outcomes (e.g. ex situ conservation, risky translocations to theoretically suitable future areas; Cunningham, 1996; Dawson, Jackson, House, Prentice, & Mace, 2011; Weeks et al., 2011). Furthermore, the effects of anthropogenic and climatic drivers can be easily confounded, thereby hindering the assessment of their relative roles in taxon current conservation status, especially when analysing only current data that implies, at best, 50–60 years of continued surveillance of species occurrences (Bradshaw & Lindbladh, 2005; Li et al., 2014; Lima-Ribeiro et al., 2013). Hence, it is crucial that the potential and current conservation status of threatened species are correctly assessed to facilitate the design and implementation of effective conservation and management plans, and to focus efforts on the most serious threat factors (Bolten et al., 2011).

Although conservation biology is usually based on current observational (short-term) data, an increasing number of studies are now integrating long term/palaeobiological data into analytical frameworks (Birks, 2012; Davies & Bunting, 2010; Louys, 2012; Maclean et al., 2014; Millar & Brubaker, 2006; Willis et al., 2007). This approach can help to characterize the potential taxon status and baseline/pre-anthropogenic conditions of endangered species in the context of their taxon history (Figure 1). Furthermore, these baseline conditions can be used as the objective for restoration plans and conservation policies and to select target species for conservation, replacing criteria based purely on short-term data (IUCN Species Survival Commission, 2012). Species with current conservation problems caused by anthropogenic factors but with an expansive phase prior to human impact (and with a predictable capacity to survive in the future) can be protected with the cheapest, more feasible and effective conservation measures. The efficacy of conservation efforts for species with current conservation problems unconnected with

human impacts (and with a predictable limited capacity to survive in future ecosystems even without anthropogenic perturbations) is unpredictable and such efforts should be limited to local and

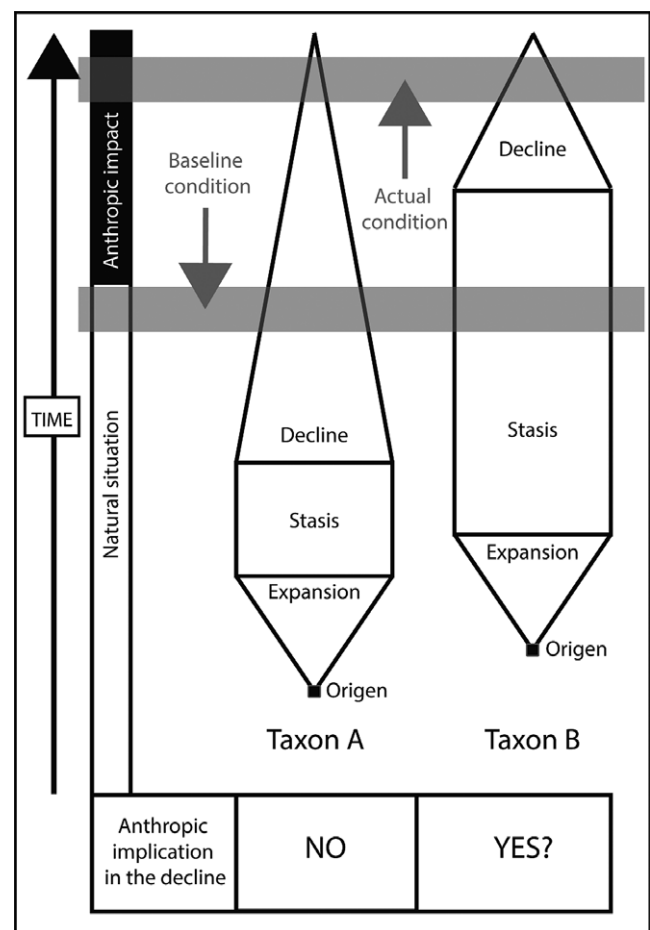


FIGURE 1 Characterizations of two alternative baseline conditions for a declining taxon history and the potential role of anthropogenic drivers. Declining in species A is due to climatic drivers and starts before human impacts, which correspond with a declining baseline condition. However, declining in species B starts simultaneously to human impacts and thus could be due (at least in part) to human activities, which correspond with a baseline condition of stasis. Conservation and recovery plans to limit human impact on ecosystems to restore the baseline condition would be effective for species B but useless for species A, which is also affected by climatic factors

inexpensive initiatives (micro-reserves, ex situ conservation, etc.) (Louys, 2012; Willis et al., 2007). Hence, it is important that better quality data and methodologies are assembled to assess the baseline conditions of endangered species. A potential source of error in long-term datasets comes from important spatio-temporal biases in the fossil record, limited research funding, or the limited interest of palaeontologists in the Holocene, a crucial period for defining baseline conditions (Jackson & Johnson, 2001; Louys, 2012).

Statistical and computational tools that relate species occurrence/abundance to environmental variables (species distribution models or SDMs) (Guisan & Zimmermann, 2000) are widely used to study distribution drivers and are increasingly being used in palaeoecology to address the limitations of the fossil record (Maguire, Nieto-Lugilde, Fitzpatrick, Williams, & Blois, 2015). Hence, the combination of a dynamic approach—an analysis of multi-temporal data (i.e. both current and long-term data)—and the analytical power of SDMs provides deeper insights into potential taxon status and help disentangling the relative roles of distribution drivers and their potential impact as threat factors.

Cabrera's vole *Microtus cabreræ*, Thomas 1906 is a good example of a species that will benefit from such integrated study. This endemic Cricetidae of the Iberian Peninsula only lives in tall perennial meadows associated with moist soils, which provide protection from predators and extreme weather, as well as a guaranteed food supply (i.e. green grass). Its distribution is currently small and fragmented and it is classified as Vulnerable to extinction in Spain and Portugal (Pita, Mira, & Beja, 2014).

The study of its current conservation status is based on two main approaches. Short-term data highlighting the effects of human pressure (habitat losses through the expansion/intensification of croplands and animal husbandry) in combination with the species' stenotopy as the principal threat factors (Pita et al., 2014). Conversely, long-term data have been used to tentatively reconstruct its taxon history, with its emergence during the Marine Isotope State 5 (130–71 ka BP), expansion in the Early Holocene (10.5–7.5 ka BP), maximum/stasis in the Mid-Holocene (7.5–5 ka BP) and a decline in the Late Holocene that led to its current situation (Garrido-García & Soriguer-Escofet, 2012; Laplana & Sevilla, 2013; López-Martínez, 2003, 2009). Three hypotheses have been proposed to explain the historical origin of this decline: (1) increased aridity at the beginning of the Subboreal period (5.3 ka BP; López-Martínez, 2003, 2009), (2) expansion and intensification of agriculture and animal husbandry during the Subatlantic period (2.5 ka BP; Garrido-García & Soriguer-Escofet, 2012) and (3) a combination of these two processes (Laplana & Sevilla, 2013).

A recent genetic study at the population level that determined the effective female population sizes (N_{ef}) during the Holocene (Barbosa et al., 2016) suggest that its populations (number of individuals) increased until 1.0–2.0 ka BP. This result is consistent for the two phylogenetic lineages of the species (west and east lineages) and for the species as a whole (see Figure 2, extracted from Barbosa et al., 2016). Although this chronology supports the hypothesis of decline due to expansion and intensification of agriculture and animal

husbandry, it does not directly address the potential drivers of such change.

Hence, the relative impact of anthropogenic and climatic drivers on *M. cabreræ* is still unresolved due to the difficulty in disentangling these drivers from short-term data and the scarcity of fossil/archaeozoological records for the Subboreal and Subatlantic periods, which limits our ability to date the start of the decline. Furthermore, its fossil records show notable biases: (1) in the spatial distribution of records between the eastern and the western part of its current range due to the unequal presence of appropriate substrates for fossilization (see a review in Laplana & Sevilla, 2013) and (2) in the sampling effort of microfauna in sites of the different historical periods and regions (Garrido-García, 2008; Garrido-García & Soriguer-Escofet, 2012; Laplana & Sevilla, 2013).

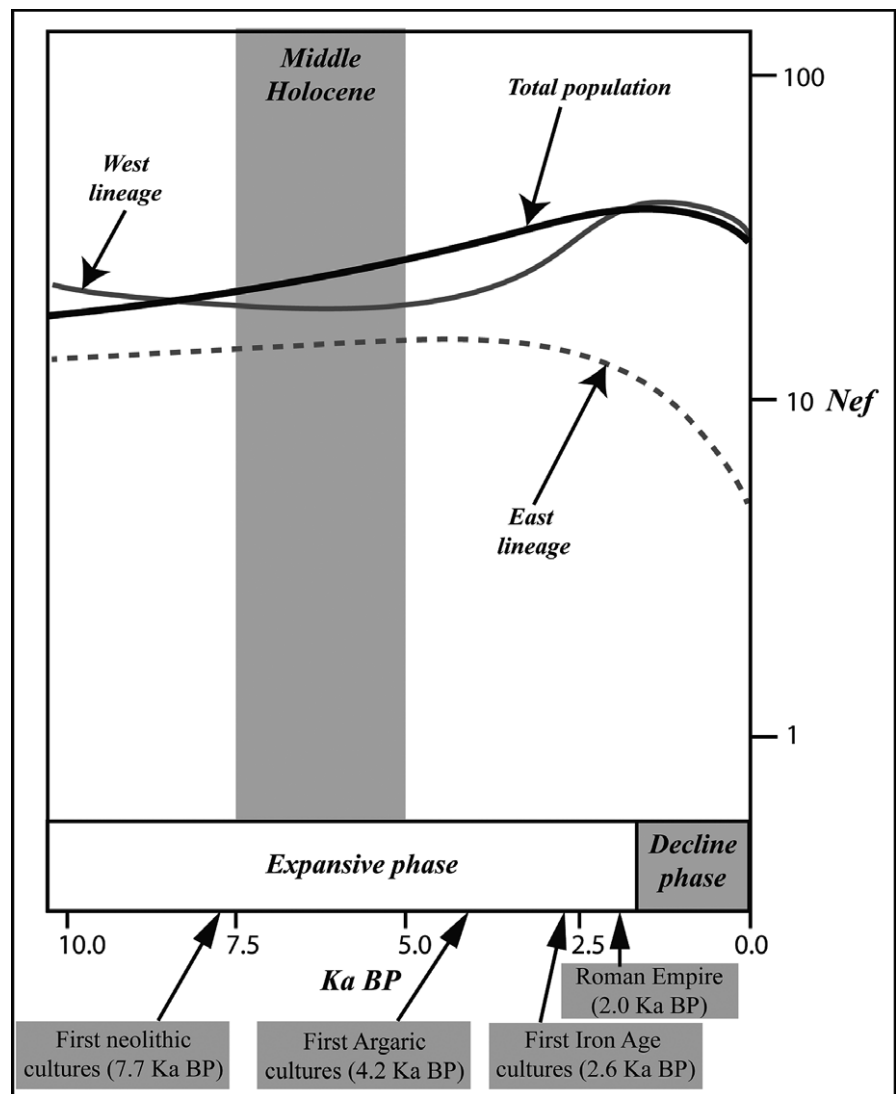
Here, we combine short- and long-term data with SDMs to characterize both the baseline conditions and potential status of *M. cabreræ* in the context of its taxon history, and to understand the processes and drivers affecting the decline in its distribution since the Mid-Holocene (~6 ka BP). More specifically, we aimed to clarify: (1) whether its actual distribution is constrained by current climatic conditions (namely aridity) or by anthropogenic pressure, (2) the occupancy of its potential spatial distribution and (3) how its potential distribution has changed over the past 6 ka. Answering these questions will help to disentangle the relative roles that humans and climate have played in biodiversity patterns and to improve the characterization of the baseline conditions of this threatened species, which in turn, will enable us to define the species' threat factors and optimize conservation plans.

2 | MATERIALS AND METHODS

We compared the effects of climatic and anthropogenic pressure as a means of determining their relative importance in the current realized distribution of *M. cabreræ*. Then, to evaluate the occupancy and long-term changes in its potential distribution, we fitted an ensemble of SDMs based only on climate variables and projected to climate conditions at current (Actual Potential Condition, APC) and at approximately 6 ka BP (Mid-Holocene Potential Condition, MHPC) that were, respectively, evaluated using a comprehensive and exhaustive set of both current (Actual Condition, AC) and Mid-Holocene fossil data.

If climate factors were responsible for its decline, (1) they should have a stronger effect than anthropogenic factors when explaining its current distribution, (2) the areas of occupancy in its APC and AC will be similar and (3) the area of occupancy in APC will be smaller and more fragmented than in the MHPC. Conversely, if anthropogenic variables had a greater effect, (1) they will be more prominent in explaining the current potential distribution, (2) the areas of occupancy in APC will be bigger than in AC and (3) the occupancy of APC will not be any smaller or more fragmented than in MHPC.

FIGURE 2 Estimated evolution of the effective population size of *Microtus cabreræ* (Number of effective females— N_{ef} —, thousands in logarithmic scale; Y axis) in the Holocene (ka BP; X axis) determined for the total population and for the populations included in the west and east lineages (Iberian Peninsula and southern France). Main historic events pinpointed after Almagro-Gorbea (2014). Lines are simplified versions of the Bayesian skyline plots based on *cyt-b* data (Barbosa et al., 2016). The evolution of the total population shows a continuous growth until the 2nd millennium BP, and a subsequent reduction (expansive and decline phases indeed over the X axis). The behaviour of the East lineage is similar, but with an earlier transition between the expansive and decline phases (4th millennium BP). The West lineage shows a gradual decline until the Mid-Holocene, a fast growth between the Mid-Holocene and the 3rd millennium BP, and a later decline



2.1 | Study area and distribution data

The study area encompasses both the species' current and Mid-Holocene distribution areas (Iberian Peninsula and southern France; 12.66°W–9.92°E; 33.42°N–47.42°N; Figure 3) (Garrido-García & Sorriquer-Escofet, 2012; Garrido-García et al., 2013; Laplana & Sevilla, 2013). Furthermore, to refine the analysis of the changes in potential distribution, we divided the area into four regions according to the population nuclei defined in the species' current distribution (Betic, Luso-Carpetanian, Pirenaic-Occitanan, Montiberican; Figure 3) (Garrido-García et al., 2013).

Occurrence data during the Mid-Holocene ($n = 27$; all originally georeferenced using UTM coordinates at 1×1 m resolution) were compiled from reviews of its fossil records (Garrido-García & Sorriquer-Escofet, 2012; Laplana & Sevilla, 2013), selecting sites of the Neolithic period (7.5–5.1 ka BP) that encompass most of the Mid-Holocene (Almagro-Gorbea, 2014; Borzenkova, 1990) (list of sites in Table S1.1, Appendix S1). Because available Mid-Holocene climate estimations correspond to 100 years average around 6.0 ka BP

(Varela, Lima-Ribeiro, & Terribile, 2015), we further searched for strata with *M. cabreræ* remains with calibrated C^{14} dates (Table S1.2, Figure S1 in Appendix S1). Among the 20 sites with chronostratigraphic information, nine have estimated age ranges (1σ) for our target species overlapping (at least partially) with the range 5.75–6.25 ka BP, and among those seven overlap with the most restrictive age range 5.9–6.1 ka BP. By doing so, we aim to improve temporal matching between palaeoclimate simulation and palaeorecords, which is important because of the climatic instability during the Mid-Holocene (Zielhofer et al., 2017) and the uncertainty in palaeoclimate simulations (Varela et al., 2015).

Current records ($n = 481$) in UTM coordinates at 10×10 km resolution were extracted from a current distribution map (Garrido-García et al., 2013), updated with new data (Belenguer et al., 2016; Mestre et al., 2015; Vale-Gonçalves & Cabral, 2014; Barbosa, *pers. comm.*). This resolution more accurately represents *M. cabreræ* distribution because differential sampling efforts among regions result in an uneven spatial density of samples at finer resolution (Garrido-García et al., 2013), and many records derive from

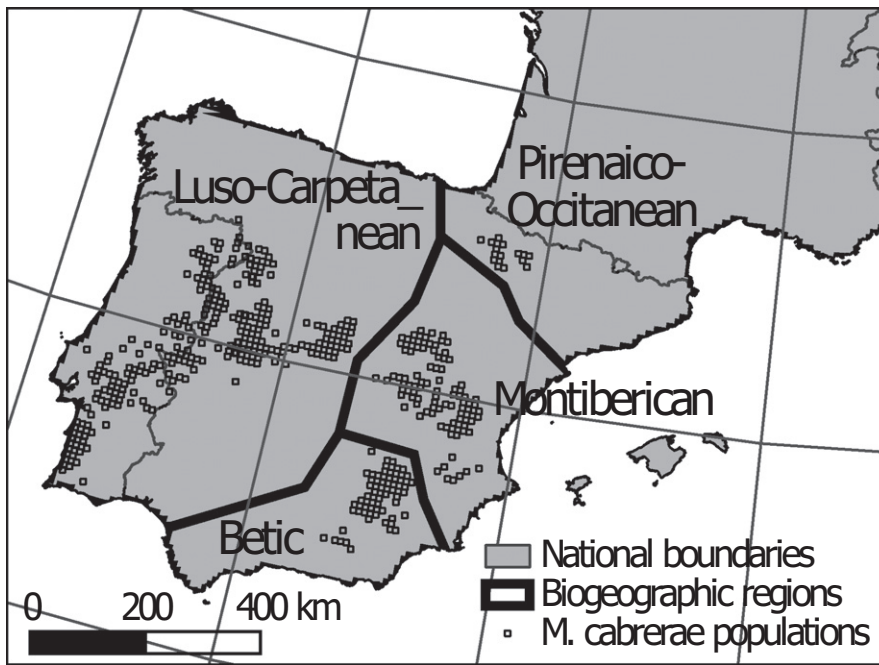


FIGURE 3 Distribution map for current populations of *Microtus cabreræ* (squares) in the Iberian Peninsula (Spain and Portugal; SW Europe). The map also depicts boundaries of four biogeographical regions: Luso-Carpetanean, Pirenaico-Occitanean, Montiberican and Betic. Map is projected using ED50 datum and UTM zone 30 N

owl pellets (e.g. Vale-Gonçalves & Cabral, 2014), which indicate location of owls nests rather than the actual rodent location. Given that these data are presence-only, we complemented them with 2,000 random pseudo-absences (Barbet-Massin, Jiguet, Albert, & Thuiller, 2012). A sensitivity analysis equalizing the number of presences and pseudo-absences, to control for biases due to pseudo-absences number, returned identical results (Appendix S2).

All fossil and current occurrence data were then projected onto a longitude–latitude coordinate system for consistency with environmental variables (see below).

2.2 | Environmental variables

2.2.1 | Climate

Current (1950–2000) and Mid-Holocene (~6 ka BP) climate data were downloaded from the WorldClim database 1.4 (<http://www.worldclim.org>; Hijmans, Cameron, Parra, Jones, & Jarvis, 2005) at 5-arcmin resolution (~10 km) in longitude–latitude coordinate system. Mid-Holocene climate reconstructions were downloaded for two Ocean Atmospheric General Circulation Models (OA-GCM): CCSM4 and MIROC-ESM. Of the 19 bioclimatic variables, for both periods, we selected temperature seasonality (Tsea), minimum temperature of the coldest month (Tmin) and precipitation seasonality (Psea). To account for aridity (hypothesized as being responsible for the decline of *M. cabreræ*; López-Martínez, 2003, 2009; Laplana & Sevilla, 2013), we calculated an aridity index (AI) using monthly precipitation and temperature values available in WorldClim, and defined as the fraction of the annual potential evapotranspiration (ETP) compensated by the annual precipitation ($AI = ETP/AP$) (details in Appendix S3).

2.2.2 | Human pressure

We used the human influence index (HII; Wildlife Conservation Society & Center for International Earth Science Information Network, 2005); however, given that this index is based purely on urban/transport-related infrastructures, we also used data that represent the proportion of land in the year 2,000 devoted to cropland (cropland; Ramankutty, Evan, Monfreda, & Foley, 2010a) or livestock farming (pastures; Ramankutty, Evan, Monfreda, & Foley, 2010b). To separate the potential importance of irrigated and rain-fed crops, we used the global map of percentage of irrigated land around the year 2005 (Siebert, Henrich, Frenken, & Burke, 2013). By multiplying this layer by croplands, we estimated the proportion of irrigated croplands (“irrigated”) and, by subtracting irrigated from the croplands, we calculated the proportion of rain-fed croplands (“rainfed”). Croplands, pastures and irrigated variables were all downloaded at 5-arcmin resolution. HII, which is only available at 0.5-arcmin, was downscaled by averaging the value of all 0.5-arcmin cells within each 5-arcmin cell.

Pairwise correlations and the analysis of the variance inflation factor (VIF) between all climatic and anthropogenic variables (Appendix S4) revealed a lack of collinearity ($\rho < 0.75$ in all pairwise comparisons) and multicollinearity ($VIF < 3.3$ for the eight variables).

2.3 | Drivers of current realized distribution

To analyse the effect of the drivers on the current distribution, we fitted multiple binomial generalized linear models (GLMs) using a logit link function. First, we fitted eight GLMs relating current presence–absence to each environmental variable (single models). Then, we fitted three multivariate GLMs, with (1) all four climatic variables

TABLE 1 Multiple predictor models to explain *Microtus cabreræ*'s current distribution (Iberian Peninsula and southern France) (presences $n = 481$; pseudoabsences $n = 2,000$), using generalized linear models with a logit link function. Semi-standardized coefficients are given in parentheses. Single models represent the isolated effect of each predictor variable on the dependent variable (i.e. *M. cabreræ*'s distribution), climate model accounts for the multivariable effect of all climatic variables, anthropogenic model accounts for the combined effect of all anthropogenic variables, whereas the full model account for the combined effect of climate and anthropogenic variables. Multivariable models were selected through a stepwise procedure based on minimum residual autocorrelation. Spatial autocorrelation was accounted for in full model with SF (Full + SF) by including spatial eigenvector mapping (SEVM) as predictor variables. Climate predictor variables are temperature of the coldest month (Tmin), temperature seasonality (Tsea), aridity index (AI) and precipitation seasonality (Psea); anthropogenic variables include human influence index (HII), irrigated crops (Irrig.), rainfed crops (Rainf.) and pastures (Past.). All predictor variables did not show co- or multico-linearity (see Tables S4.1 and S4.2 in Appendix S4), except Tmin and Psea (Pearson = 0.74)

Variables	Single models		Climate model		Anthropogenic model		Full model		Full + SF model	
	Coef.	<i>p</i>	Coef.	<i>p</i>	Coef.	<i>p</i>	Coef.	<i>p</i>	Coef.	<i>p</i>
Intercept			-4.035	***	-0.325	n.s.	-4.299	***	-0.415	***
Climatic										
Tmin	-0.005 (-0.051)	**	-0.010 (-0.108)	*	—	—	—	—	—	—
Tsea	0.000 (0.123)	***	0.000 (0.071)	*	—	—	0.000 (0.107)	***	0.005 (2.812)	***
AI	0.666 (0.070)	***	0.380 (0.040)	n.s.	—	—	1.490 (0.156)	***	-0.948 (-0.187)	n.s.
Psea	0.002 (0.011)	n.s.	0.024 (0.117)	**	—	—	0.018 (0.091)	***	0.067 (0.718)	***
Anthropogenic										
HII	-0.050 (-0.123)	***	—	—	-0.032 (-0.098)	***	-0.038 (-0.116)	***	0.007 (-0.056)	n.s.
Irrig.	-10.05 (-0.306)	***	—	—	-6.462 (-0.197)	***	-8.052 (-0.245)	***	-7.434 (-0.375)	**
Rainf.	-1.389 (-0.130)	***	—	—	-0.757 (-0.071)	***	-1.723 (-0.161)	***	-2.872 (-0.458)	***
Past.	0.279 (0.012)	n.s.	—	—	0.226 (0.009)	n.s.	0.837 (0.035)	n.s.	1.979 (0.208)	n.s.
N° Spatial filters									67	
Pseudo-R ²			0.135		0.189		0.279		0.491	
AIC			2371.65		2304.45		2190.15		929.175	
minRSA			2.484		0.897		0.711		0.005	
Moran's I										
<i>k</i> = 1			0.576		***		0.288		***	
<i>k</i> = 10			0.488		***		0.218		***	
<i>k</i> = 50			0.345		***		0.155		***	
<i>k</i> = 100			0.241		***		0.114		***	

Signif. codes: ***<.001; **<.01; *<.05.

Values in brackets are the semi-standardized coefficients.

(climatic model), (2) all four anthropogenic variables (anthropogenic model) and (3) all eight climatic and anthropogenic variables (full model). The full (saturated) model was fitted in a step-wise procedure using the Akaike information criterion (AIC) to select the optimum model ($\Delta AIC < 2$). As the final full model exhibited high spatial autocorrelation on the residuals (Table 1), which can affect parameter estimation, we calculated spatial filters (SF) for the complete set of presence-pseudoabsence data, removing those SF correlated ($r > .5$) with any of the variables. Then, starting with the full model, we performed a new stepwise regression by including a spatial filter (SF) at each step until spatial autocorrelation was effectively removed (full + SF model). Spatial autocorrelation here was measured as the minimum residual spatial autocorrelation (minRSA) by summing the absolute Moran's I values in the first 20 distance classes (50-km increments) of the correlogram (following Kissling & Carl, 2008). In addition, Moran's I was calculated with a different number of neighbours ($k = 1, 10, 50, 100$) for all models.

Finally, to obtain comparable values for all variables, we semi-standardized all the model coefficients (following eq. 2 in Menard, 2004). Although this approach does not consider variation in the dependent variable, we were interested in comparing coefficients within the same model rather than between models with different response variables.

2.4 | Current and Mid-Holocene potential distributions

To estimate APC and MHPC distributions, we fitted SDMs relating current occurrences to climate variables only. To reduce potential sampling biases and pseudoreplication, we subsampled the occurrence data by applying an environmental filter (Varela, Anderson, García-Valdés, & Fernández-González, 2014), which randomly selects one presence/absence data from each group of presences/absences with similar climatic conditions. For each subsample, 30% of the data

were held for testing purposes and 70% for training the models. To account for uncertainties in SDMs (Figure 4), we used an ensemble approach (Araújo & New, 2007) that combined different sources of uncertainty: random subsampling when applying environmental filters, modelling techniques and climate simulations in the case of Mid-Holocene conditions. To do so, we applied the environmental filter 50 times and used eight modelling algorithms: bioclim, Mahalanobis distance, generalized linear models (GLM), generalized additive models (GAM), random forest, multivariate adaptive regression splines (MARS), boosted regression trees (BRT) and Maxent (Phillips, Anderson, & Schapire, 2006). We used a binomial family with a logit link function to fit GLMs (fitted with quadratic terms for all predictor variables), GAMs (fitted with smoothing functions with four degrees of freedom) and MARS. BRT were fitted using a Bernoulli distribution, allowing three degrees of interaction between predictor variables with the `gbm.perf` function (R package “gbm”; Ridgeway, 2007) to calculate the number of trees used in each model. Maxent was fitted with the default parameters. In total, we fitted 400 models (50 subsamples \times 8 algorithms).

All the models were projected onto current and Mid-Holocene climatic conditions, which gave 400 predictions for current conditions and 800 for Mid-Holocene conditions (400 models \times 2 OA-GCMs). To account for uncertainty and circumvent the heterogeneity of outputs from the different modelling algorithms (although all are on the same scale [0–1], some provide probabilities while others calculate suitability indices), we did not calculate the average prediction. Instead, grid cells in the model projections were subsequently classified as suitable/unsuitable (1/0) using the model-subsample-specific threshold that maximizes the sum of sensitivity and specificity (e.g. those that give the best balance between correctly predicted presences and absences). These binary predictions were then combined (model ensemble) calculating the means and confidence intervals for each period. The resulting maps are interpreted as indicators of the consensus level between subsamples, algorithms and OA-GCMs (in the case of the Mid-Holocene), with high (>0.5) and low consensus (<0.5).

The current average prediction from the model ensemble (mean of individual binary predictions from all models) was evaluated 50 times (50 random subsets when applying environmental filters) using two approaches: (1) the area under the curve of the receiver operating characteristic plot (AUC), a threshold independent measure of the probability that a given model will assign a higher prediction to a known presence over random points in the study area. This is widely used in SDMs studies but is known to be affected by the prevalence of the modelled species; and (2) the true skill statistics (TSS), a threshold-dependent measure unaffected by prevalence (Allouche, Tsoar, & Kadmon, 2006). Mid-

Holocene predictions were evaluated by comparing output from model ensemble for that period with the three fossil datasets (7.5–5.1 ka BP, 6.25–5.75 ka BP and 6.1–5.9 ka BP) using the continuous Boyce index (Hirzel, Le Lay, Helfer, Randin, & Guisan, 2006), which has been proposed to evaluate models when presence-only data are available. This is especially important for fossil data where assumptions regarding the use of pseudo-absences for model evaluation are less reliable.

To compare AC with APC, and APC with MHPC, we used “SDMTools” for R (Van Der Wal, Falconi, Januchowski, Shoo, & Storlie, 2014) to measure the surface of suitable areas (model ensemble >0.5) in each period for the whole study area (total), for each region (Figure 3) and for all suitable and isolated patches. We estimated the actual degree of occupancy as the ratio of AC (from the actual distribution) and APC (from the model ensemble). We tested for significant differences in suitable areas between regions using a χ^2 -test. To analyse long-term changes, we compared distributions in APC and MHPC by analysing changes in total and regional areas of occupancy and in fragmentation levels, shifts in distribution and the importance of the edge effect, that make populations more vulnerable to demographic and environmental stochasticity by increasing the isolation of populations and decreasing genetic variability, as well as the amount and quality of available resources (Bahn, O’Connor, & Krohn, 2006). Shifts in distributions were tested by analysing the potential distribution area within each defined region (Figure 3) using a χ^2 -test. We measured the degree of fragmentation as the largest isolated patch/total suitable area ratio, and the edge effect using the area/perimeter ratio (A/P ratio) in each isolated patch respectively. We assessed differences in the number of isolated patches between APC and MHPC using a χ^2 -test, whereas differences in fragmentation and edge effect were evaluated using a Mann–Whitney *U* test.

Manipulation (cropping and projecting) and calculations of spatial data (occurrences and environmental variables) were performed using QGIS software (QGIS Development Team, 2012). All model fitting and projections, as well as the subsequent statistical analysis, were performed in R 3.2.2 (R Core Team, 2015).

3 | RESULTS

3.1 | Drivers of current distribution

Despite differing significance for some of the variables, single, climatic, anthropogenic and both full models all provide consistent results regarding the effect of each variable on the current distribution of *M. cabreræ* (Table 1). Of the climatic drivers, *M. cabreræ* was

FIGURE 4 Binary suitability (suitable/unsuitable) maps of *Microtus cabreræ* according to model ensemble for current conditions (left column) and Mid-Holocene (right column) in the study area (Iberian Peninsula and southern France). Maps represent lower confidence interval (lower row; 95% confidence level), mean (middle row) and higher confidence interval (higher row; 95% confidence level) of suitability from all SDMs in the ensemble. Those maps are calculated using 50% of consensus (>0.5) as threshold to differentiate between suitable and unsuitable areas from continuous predictions as depicted in Appendix S5. Maps also depicts known presences of *M. cabreræ* at each period according to current observations or fossil records. Maps are projected using ED50 datum and UTM zone 30 N



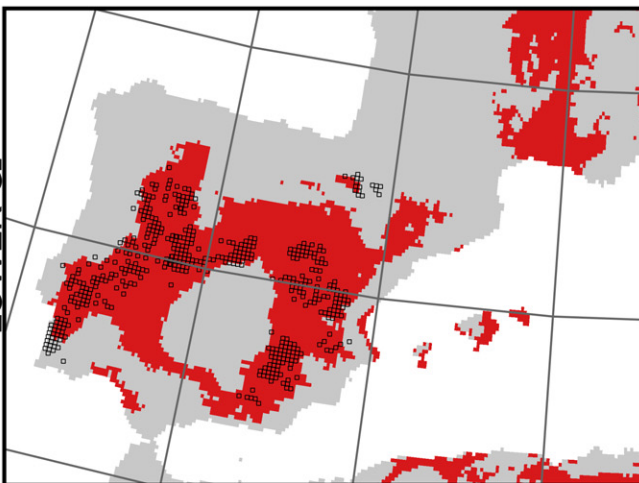
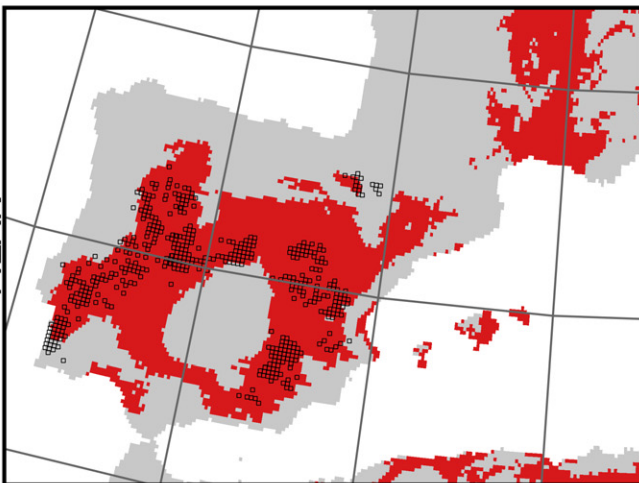
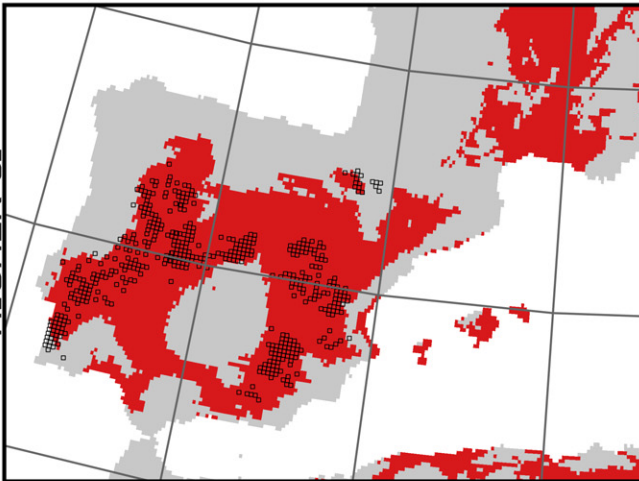
PRESENT

MID-HOLOCENE

HIGHER CI

MEAN

LOWER CI



Presences

- Current
- 7500-5100 yrs BP
- 6250-5750 yrs BP
- 6100-5900 yrs BP

Suitability

- ◻ < 0.5
- ◼ ≥ 0.5

0 200 400 km



negatively affected by cold winters (Tmin) and positively by seasonality (Tsea, Psea). AI had a positive effect in all models except full + SF (non-significant). Of the anthropogenic drivers, urban development (HII), irrigated and rain-fed croplands had a negative significant effect (except HII, whose effect is non-significant in full + SF), whereas pastures had a positive but non-significant effect. All variables except Tmin were selected by the step-wise regression into the full model. In the full + SF model, which is not affected by spatial autocorrelation, climatic factors were more important than anthropogenic factors (see semi-standardized coefficients, Table 1) and significant climatic variables (Psea, Tsea) had a positive effect, whereas significant anthropogenic variables (rain-fed and irrigated crops) had a negative effect.

3.2 | Current potential distribution and actual occupancy (APC versus AC)

The estimates of the current potential distribution using the model ensemble reflected the actual spatial distribution, with 94.18% of populations being included in the suitability map (Figure 4, Figure S5; Appendix S5). In fact, the ensemble showed high performance when estimating current distribution ($AUC_{test} = 0.868 \pm 0.008$; $TSS_{test} = 0.642 \pm 0.020$) with a low level of overfitting ($AUC_{test} - AUC_{train} = -0.007 \pm 0.010$; $TSS_{test} - TSS_{train} = 0.018 \pm 0.022$). However, actual populations only occupy 12.80% of the current potential distribution and the distribution patterns between APC and AC were significantly different ($\chi^2_7 = 17379.50$, $p < .01$), with lower occupancy in the Pirenaic-Occitanan region (1.47%) than in the Montiberican (13.13%), Betic (18.74%) or Luso-Carpetanian regions (20.11%) (Table 2).

3.3 | Mid-Holocene potential distribution and comparison with current potential distribution

Overall, the model ensemble predicted the Mid-Holocene fossil records (Figure 4 and Figure S5 in Appendix S5) well. This

TABLE 2 Realized actual distribution (AC), potential actual distribution (APC) and potential Mid-Holocene distribution (MHPC) areas (squared kilometres) of *Microtus cabreræ* for each of the four biogeographical regions in the study area (Iberian Peninsula and southern France): Betic, Luso-Carpetanian, Pirenaic-Occitanan and Montiberican. The differences between regions for all distributions (AC, APC and MHPC) were significant (***: $<.001$). The total and mean areas for all regions are also given

Region	AC	APC	MHPC
Betic	7000	37363.07	17791.23
Luso-Carpetanian	29300	145737.71	116482.88
Pirenaic-Occitanan	1700	115746.80	183417.95
Montiberican	10100	76942.87	29752.50
Differences between regions	913758.10***	70766.99***	209906.46***
Total	48100	375798.45	347444.56
Mean	12025	93947.61	86861.14

agreement is also confirmed by statistical evaluation with the three fossil data sets (Boyce index: 7.5–5.1 ka BP = 0.948; 6.25–5.75 ka BP = 0.839; 6.1–5.9 ka BP = 0.790). However, it failed to capture some presences in the Betic mountains (SE Spain), Central System Mountains (central Iberian Peninsula) and Rhone valley (southern France) (Figure 4).

TABLE 3 Fragmentation analysis of the actual potential distribution (APC) and Mid-Holocene potential distribution (MHPC) of *Microtus cabreræ* (Iberian Peninsula and southern France). The parameters analysed include the number of disjoint patches (# disjoint patches), fraction of greatest patch area (Fract. Great. Patch), patch area and patch AP ratio. Means and coefficients of variation (CV) of all patches are given for patch area and AP ratio; differences were tested using a Mann–Whitney *U* test

Parameter	APC	MHPC
# disjoint patches	41	4
Fract. Great. Patch	0.71	0.99
Patches area		
Mean	6725.30	86861.14
CV	4.66	1.99
Mann–Whitney <i>U</i>	$U = 48.00$; $W = 909.00$; $z = -1.356$; $p = .175$	
Patches AP ratio		
Mean	4.19	9.25
CV	1.33	1.22
Mann–Whitney <i>U</i>	$U = 45.00$; $W = 906.00$; $z = -1.476$; $p = .140$	

Significant differences arose when comparing the MHPC and the APC. The APC area is bigger than MHPC area (Table 2; $\chi^2_1 = 1111.45$; $p < .01$), the fraction of the total area included in the main population core is smaller and the potential distribution is more fragmented in APC than in MHPC ($\chi^2_1 = 29.28$; $p < .01$) (Table 3). Differences were also significant in their spatial distribution ($\chi^2_7 = 45658.33$; $p < .01$), with shifts in all regions (Table 2), especially from the Pirenaic-Occitanan (at MHPC) to the other regions (at APC). However, there were no differences in the variability in size or A/P ratio of the patches (Table 3).

4 | DISCUSSION

4.1 | Actual condition: The role of climatic and anthropogenic factors

Given *M. cabreræ*'s stenotopy (Pita et al., 2014), the importance of the factors configuring its distribution can be partially understood by its role in the habitats themselves. Although these grasslands constitute transient successional states in a vegetation series linked with

forested climaxes (Rivas-Martínez, 1987), they are ecologically related to the steppe grasslands that are usually associated with high levels of thermal seasonality (continental climates) (Rivas-Martínez, 2011). The plants that dominate these habitats (*Brachypodium phoenicoides*, *Scirpoides holoschoenus*, *Agrostis castellana*) have a marked hygro-edaphic dependence, but need temporary low phreatic levels in summer. In the Mediterranean climate, low rainfall seasonality implies wetter summers (dry period being reduced or completely disappearing), which subsequently leads to habitats dominated by *Carex* spp., with less nutritional value for *M. cabreræ* (Costa Pérez & Valle Tendero, 2005; Pita et al., 2014). In fact, an ad hoc analysis (Appendix S6) shows that the vegetation series associated with *M. cabreræ*'s habitats (Pita et al., 2014; Rivas-Martínez, 1987, 2011) in Spain (48.85% of the study area) experience greater rainfall and thermic seasonality than the rest of the territory.

The negative effect of anthropogenic variables in its current distribution indicates that habitat losses due to agricultural expansion is most likely the main reason for the Late Holocene and current decline in *M. cabreræ* populations, which are confined in cultivated areas to natural grasslands associated with crop borders, road verges or the banks of watercourses. The linear geometry of these patches (low A/P ratio) generates negative edge effects, increasing the impact of disturbances and reducing the survival rates of populations (Pita, Mira, & Beja, 2006; Santos, Mathias, Mira, & Simões, 2007). In contrast to natural vegetation, croplands are a very unfavourable landscape matrix that act as a barrier against the genetic and demographic fluxes, which are fundamental for the viability and the recovery of extinct/damaged populations (Pita et al., 2006).

Likewise, irrigated crops involve greater landscape transformation than rain-fed crops, and the intense and repetitive destruction of semi-natural vegetation in fallow areas (characteristic of irrigated croplands) favours therophytic communities that are unsuitable for *M. cabreræ* and thus increase the local extinction risk (Santos et al., 2007). However, the lower productivity of rain-fed croplands hamper intense landscape transformation and reduce the frequency of anthropogenic perturbations, which thus allows *M. cabreræ* populations to survive on steep hillsides or in lowlands too humid to support agriculture.

4.2 | SDM predictive ability and changes in potential distribution

The low overfitting levels of model ensemble and its good performance when predicting both current and fossil records suggest that MHPC potential distribution (Figure 4; and Figure S5 in Appendix S5) might be reliable. Despite strong predictive performance, the model failed to identify the occurrence of some fossil records. Other studies have found similar problems and usually attribute this to uncertainty and errors in palaeoclimate reconstruction, changes in realized species niches, or inability of SDMs to capture realized niches (McGuire & Byrd Davis, 2013; Veloz et al., 2012). In our study, however, false negatives (fossil records

predicted as absences) are predicted as suboptimal but not completely unsuitable (Figure S5 in Appendix S5). Furthermore, those situations are concentrated in mountainous regions with greater environmental heterogeneity at smaller spatial scales. Hence, rather than by any methodological outcome, our results could be caused by the presence of microrefugia and/or a plastic response of *M. cabreræ* to suboptimal macroclimatic conditions (Millar & Brubaker, 2006), thereby ensuring the survival of populations during the Mid-Holocene in previously occupied places (see pre-Mid-Holocene distribution in Garrido-García & Soriguer-Escofet, 2012 and Laplana & Sevilla, 2013).

Unfortunately, the scarcity of fossil data in the Luso-Carpethian region because of a paucity of calcareous substrates and karst areas, combined with general biases in the detection and determination of micromammals remains in the Holocene sites of the Iberian Peninsula (see Section 1), prevent an empirical validation of the estimated potential distribution in the western part of the study area.

The most accepted hypothesis explaining the current small fragmented distribution of *M. cabreræ* is that climatic conditions became less favourable (increase in aridity) during the Late Holocene. This hypothesis implies that human pressure only played a secondary role that is restricted to (sub)actual population declines (López-Martínez, 2003, 2009; Pita et al., 2014). Our results support the alternative hypothesis (Garrido-García & Soriguer-Escofet, 2012) that climate change during the Late Holocene would have led to an increase in the potential distribution (Figure 4, Table 2). Aridity does not have a constraining role in the distribution of this rodent (Table 1) because distribution changes from MHPC to APC and from APC to AC reveal a continuous shift from low aridity regions (Pirenaic-Occitanian) to others of greater aridity (Betic, Montiberian and Luso-Carpetanian; see aridity map in Figure S3 in Appendix S3 and current versus Mid-Holocene climate comparison in Appendix S4). This conclusion is corroborated by phylogenetic data of the species (Barbosa et al., 2016; Figure 2), which do not show any evidence of demographic reduction linked to the 5.3 ka BP (Atlantic-Subboreal transition) climatic crisis but, instead, a constant population increase throughout the Holocene with a more sudden decline at 1.5–2.0 ka. Furthermore, a recent archaeological review questions the ecologic effects of the 5.3 ka BP climatic crisis in the Iberian Peninsula, indicating that this degradation may not be related to an increase in aridity but to a geographical redistribution of human populations and changes in their systems of exploitation of resources (Almagro-Gorbea, 2014).

Although climatic variables can be used to explain shifts from the MHPC to APC, anthropogenic variables are still required to explain actual levels of occupancy. Our results show that current populations are clustered, in the absence of anthropogenic degradation, in the main continuous patches of the potential distribution in APC. The negative effects of agriculture would not only have an impact on actual populations but would also be the origin of the fragmentation and isolation of populations at regional level that characterize the distribution of *M. cabreræ* today.

4.3 | AC versus APC: Occupancy of the current potential distribution

Like most Arvicolinae species, *M. cabreræ* does not fully occupy its potential distributional range (McGuire & Byrd Davis, 2013). We posit that this phenomenon is a result of intense human-derived land use changes of Mediterranean landscapes since the Mid-Holocene (Quèzel & Médail, 2003), which led to habitat reduction and fragmentation. The palaeobiological record reveals a decline in its populations in southern France during the Late Holocene that culminated in its extinction by the end of the Middle Ages (Garrido-García & Soriguer-Escofet, 2012; Laplana & Sevilla, 2013). Even though a full study of *M. cabreræ* range dynamics in the Iberian Peninsula using direct fossil records is largely precluded by the lack of such records and the limitations indicated previously, some of our results do point to an earlier onset of the decline in its populations. The region with the lowest actual occupancy levels (Pirenaic-Occitanan) are also those that first experienced Neolithic colonization (Almagro-Gorbea, 2014), were the object of the most intensive exploitation during the Roman colonization (De Soto & Carreras, 2014; Duby, 1975), and have, since the Middle Ages, had the highest rates of irrigation in floodplains (Gil Olcina & Morales Gil, 1992). The same circumstances apply to the Betic and Montiberican regions (Almagro-Gorbea, 2014; Bertrand & Sánchez Viciana, 2006; De Soto & Carreras, 2014) but their complex orography ensured that agriculture was concentrated in the broadest valleys, thereby allowing *M. cabreræ* to survive in the mountainous areas. Thus, the environmental heterogeneity of these regions would allow an inelastic response to agricultural pressure that guaranteed the species' survival (Millar & Brubaker, 2006). Finally, the weak effects of the animal husbandry (Table 1) could be due to the complex relationship between the animal husbandry and the rodent, in which the positive effects of extensive management (creation and maintenance of suitable habitats) are offset by the negative effects of intensive management (extinctions in habitats with high density of livestock) (Mysterud, 2006; Pita et al., 2014; Traubaud, 1993).

4.4 | Baseline conditions and potential status of *M. cabreræ*: Implications for conservation planning

Overall, our study suggests that, without human pressure, the expansion of *M. cabreræ*'s distribution area that started after the LGM could continue (and intensify) during the Holocene, associated with a concomitant increase in population size (Barbosa et al., 2016). We note that Araújo, Guilhaumon, Rodrogues Neto, Pozo Ortego, and Gómez Calmaestra (2011) and Mestre et al. (2015) suggest a potential future decline of *M. cabreræ* due to climate change. Because we did not project our models into the future, it is not possible to decipher if such prediction corresponds to a real decrease in suitability, or to methodological differences with our models.

If *M. cabreræ* is constrained above all by increasing aridity and not by anthropogenic pressure, only limited conservation measures (ex situ conservation and microreserves) would be justifiable

(Dawson et al., 2011). However, the importance of agriculture in its current conservation status would justify investment in the design and application of a recovery plan to reduce their impact, ensuring the conservation of self-sufficient metapopulations and matching its conservation concern (i.e. vulnerable with risk of regional extinctions in Spain; Garrido-García et al., 2013; Pita et al., 2014) and legal situation (strictly protected under the 92/43/CEE Directive). This remains true regardless of future climate change impact, as climate change may synergistically act with anthropogenic threats to induce further population declines (Mestre, Risk, Mira, Beja, & Pita, 2017).

ACKNOWLEDGEMENTS

This work was funded by Spanish Ministry of Economy and Competitiveness and Andalusian Regional Government through the projects Desirè-HAR2013-43701-P (Plan Nacional I+D+I), RelictFlora-P11-RNM-7033 (Excellence Research Projects Program), RNM118 and NET829160 (EGMASA). The collaboration of Antonio Franco (Andalusian Government Environment Department) was fundamental to obtain the necessary funds.

ORCID

José Antonio Garrido-García  <http://orcid.org/0000-0003-4290-7885>

Diego Nieto-Lugilde  <http://orcid.org/0000-0003-4135-2881>

Francisca Alba-Sánchez  <http://orcid.org/0000-0003-0387-1533>

Ramón C. Soriguer  <http://orcid.org/0000-0002-9165-7766>

REFERENCES

- Allouche, O., Tsoar, A., & Kadmon, R. (2006). Assessing the accuracy of species distribution models: Prevalence, Kappa and the True Skill Statistic (TSS). *Journal of Applied Ecology*, 43, 1223–1232. <https://doi.org/10.1111/jpe.2006.43.issue-6>
- Almagro-Gorbea, M. (Ed.) (2014). *Protohistory of the far west of Europe. From neolithic to roman conquest*. Burgos, Spain: Burgos University–Atapuerca Foundation.
- Araújo, M. B., Guilhaumon, F., Rodrogues Neto, D., Pozo Ortego, I., & Gómez Calmaestra, R. (2011). *Impactos, vulnerabilidad y adaptación al Cambio Climático de la biodiversidad española. 2 Fauna de vertebrados*. Madrid, Spain: Dirección General de Medio Natural y Política Forestal-Ministerio de Medio Ambiente, y Medio Rural y Marino.
- Araújo, M. B., & New, M. (2007). Ensemble forecasting of species distributions. *Trends in Ecology and Evolution*, 22, 42–47. <https://doi.org/10.1016/j.tree.2006.09.010>
- Bahn, V., O'Connor, R. J., & Krohn, W. B. (2006). Effect of dispersal at range edges on the structure of species ranges. *Oikos*, 115, 89–96. <https://doi.org/10.1111/oik.2006.115.issue-1>
- Barbet-Massin, M., Jiguet, F., Albert, C. H., & Thuiller, W. (2012). Selecting pseudo-absences for species distribution models: How, where and how many? *Methods in Ecology and Evolution*, 3, 327–338. <https://doi.org/10.1111/j.2041-210X.2011.00172.x>
- Barbosa, S., Pauperio, J., Herman, J. S., Ferreira, C. M., Pita, R., Vale-Gonçalves, H. M., ... Searle J.B. (2016). Endemic species may have complex histories: Within-refugium phylogeography of an endangered Iberian vole. *Molecular Ecology*, 26, 951–967. <https://doi.org/10.1111/mec.13994>

- Belenguer, R., Monsalve, M. A., López-Alabau, A., Guillem, P. M., Barona, J., Belda, A., & López-Iborra, G. (2016). Nuevas aportaciones al conocimiento de la distribución del topillo de Cabrera *Iberomys cabreræ* (Thomas, 1906) en el Levante peninsular. *Galemys*, 28, 53–56.
- Bertrand, M., & Sánchez Viciana, J. R. (2006). L'irrigation du territoire de Guadix, Les grandes acequias de Sierra Nevada: l'Acequia de la Sierra. In P. Cressier (Ed.), *La maîtrise de l'eau en Al-Andalus. Paysages, pratiques et techniques* (pp. 1–49). Madrid, Spain: CNRS-Casa de Velázquez.
- Birks, H. J. B. (2012). Ecological palaeoecology and conservation biology: Controversies, challenges, and compromises. *International Journal of Biodiversity Science, Ecosystem Services & Management*, 8, 295–304.
- Bolten, A. B., Crowder, L. B., Dodd, M. G., MacPherson, S. L., Musick, J. A., Schroeder, B. A., ... Snover M. L. (2011). Quantifying multiple threats to endangered species: An example from loggerhead sea turtles. *Frontiers in Ecology and Environment*, 9, 295–301. <https://doi.org/10.1890/090126>
- Borzenkova, I. I. (1990). Climatic changes through late glacial and post-glacial. 16–0 ka BP. In V. A. Zubakov & I. I. Borzenkova (Eds.), *Global Paleoclimate of the late Cenozoic* (pp. 251–295). New York, NY: Elsevier.
- Bradshaw, R. H. W. & Lindbladh, M. (2005). Regional spread and stand-scale establishment of *Fagus sylvatica* and *Picea abies* in Scandinavia. *Ecology*, 86, 1679–1686. <https://doi.org/10.1890/03-0785>.
- Costa Pérez, J. C., & Valle Tendero, F. (2005). *Serie de vegetación edafohigrófila de Andalucía*. Sevilla (Spain): Junta de Andalucía.
- Cunningham, A. A. (1996). Disease risks of wildlife translocations. *Conservation Biology*, 10, 349–353. <https://doi.org/10.1046/j.1523-1739.1996.10020349.x>.
- Davies, A. L., & Bunting, M. J. (2010). Applications of palaeoecology in conservation. *The Open Ecology Journal*, 3, 54–67.
- Dawson, T. P., Jackson, S. T., House, J. H., Prentice, I. C., & Mace, G. M. (2011). Beyond predictions: Biodiversity conservation in a changing climate. *Science*, 332, 53–58. <https://doi.org/10.1126/science.1200303>
- De Soto, P., & Carreras, C. (2014). GIS and network analysis applied to the study of transport in the Roman Hispania. In N. Barrero Martín & M. J. Pérez del Castillo (Eds.), *XVIII CIAC: Centro y periferia en el mundo clásico* (pp. 733–738). Mérida, Spain: Museo de Arte Romano.
- Duby, G. (1975). *Histoire de la France rurale. I. Des origines à 1340*. Paris, France: Seuil.
- Garrido-García, J. A. (2008). Las comunidades de mamíferos del sureste de la Península Ibérica: Elementos para un análisis histórico. *Galemys*, 20, 3–46.
- Garrido-García, J. A., Rosário, I. T., Gisbert, J., García-Perea, R., Cordero, A. I., López-Alabau, A., & Sorriquer-Escofet, R. C. (2013). Revisión a nivel ibérico de la distribución del topillo de Cabrera o iberón, *Iberomys cabreræ* (Thomas, 1906). *Galemys*, 25, 35–49. <https://doi.org/10.7325/Galemys>
- Garrido-García, J. A., & Sorriquer-Escofet, R. C. (2012). Cabrera's vole *Microtus cabreræ* Thomas, 1906 and the subgenus *Iberomys* during the quaternary: Evolutionary implications and conservation. *Geobios*, 45, 437–444. <https://doi.org/10.1016/j.geobios.2011.10.014>
- Gil Olcina, A., & Morales Gil, A. (1992). *Hitos históricos de los regadíos españoles*. Madrid, Spain: Ministerio de Agricultura, Pesca y Alimentación.
- Guisan, A., & Zimmermann, N. E. (2000). Predictive habitat distribution models in ecology. *Ecological Modelling*, 135, 147–186. [https://doi.org/10.1016/S0304-3800\(00\)00354-9](https://doi.org/10.1016/S0304-3800(00)00354-9)
- Hijmans, R. J., Cameron, S. E., Parra, J. L., Jones, P. G., & Jarvis, A. (2005). Very high resolution interpolated climate surfaces for global land areas. *International Journal of Climatology*, 25, 1965–1978. [https://doi.org/10.1002/\(ISSN\)1097-0088](https://doi.org/10.1002/(ISSN)1097-0088)
- Hirzel, A. H., Le Lay, G., Helfer, V., Randin, C., & Guisan, A. (2006). Evaluating the ability of habitat suitability models to predict species presences. *Ecological Modelling*, 199, 142–152. <https://doi.org/10.1016/j.ecolmodel.2006.05.017>
- IUCN Species Survival Commission. (2012). *IUCN red list categories and criteria*. Version 3.1. International Union for Conservation of Nature (IUCN). Gland, Switzerland.
- Jackson, J. B. C., & Johnson, K. G. (2001). Measuring past biodiversity. *Science*, 293, 2401–2404. <https://doi.org/10.1126/science.1063789>
- Kissling, W. D., & Carl, G. (2008). Spatial autocorrelation and the selection of simultaneous autoregressive models. *Global Ecology and Biogeography*, 17, 59–71.
- Laplana, C., & Sevilla, P. (2013). Documenting the biogeographic history of *Microtus cabreræ* through its fossil record. *Mammal Review*, 43, 309–322. <https://doi.org/10.1111/mam.2013.43.issue-4>
- Li, X., Jiang, G., Tian, H., Xu, L., Yan, C., Wang, Z., ... Zhang Z. (2014). Human impact and climate cooling caused range contraction of large mammals in China over the past two millennia. *Ecography*, 38, 74–82.
- Lima-Ribeiro, M. S., Nogués-Bravo, D., Terribile, L. C., Batra, P., & Diniz-Filho, J. A. F. (2013). Climate and humans set the place and time of proboscidean extinction in late quaternary of South America. *Palaeogeography, Palaeoclimatology, Palaeoecology*, 392, 546–556. <https://doi.org/10.1016/j.palaeo.2013.10.008>
- López-Martínez, N. (2003). La búsqueda del centro de origen en biogeografía histórica. *Graellsia*, 59, 503–522. <https://doi.org/10.3989/graelisia.2003.v59.i2-3>
- López-Martínez, N. (2009). Time asymmetry in the paleobiogeography history of species. *Bulletin de la Société Géologique de France*, 180, 45–55. <https://doi.org/10.2113/gssgfbull.180.1.45>
- Lorenzen, E. D., Nogués-Bravo, D., Orlando, L., Weinstock, J., Binladen, J., Marske, K. A., ... Willerslev E. (2011). Species-specific responses of Late Quaternary megafauna to climate and humans. *Nature*, 479 (7373), 359–364. <https://doi.org/10.1038/nature10574>
- Louys, J. (2012). *Paleontology in ecology and conservation*. Berlin-Heidelberg (Germany): Springer-Verlag. <https://doi.org/10.1007/978-3-642-25038-5>
- Macleán, I. M. D., Suggit, A. J., Jones, R. T., Huntley, B., Brooks, S. J., Gilgillham, P. K., ... Caseldine C. J. (2014). Palaeoecological evidence to inform identification of potential climatic change refugia and areas for ecological restoration. *Natural England Commissioned Reports*, 173, 1–73.
- Maguire, K. C., Nieto-Lugilde, D., Fitzpatrick, M. C., Williams, J. W., & Blois, J. L. (2015). Modelling species and community responses to past, present and future episodes of climatic and ecological change. *Annual Review of Ecology, Evolution, and Systematics*, 46, 343–368. <https://doi.org/10.1146/annurev-ecolsys-112414-054441>
- McGuire, J. L., & Byrd Davis, E. (2013). Using the palaeontological record of *Microtus* to test species distribution models and reveal responses to climate change. *Journal of Biogeography*, 40, 1490–1500. <https://doi.org/10.1111/jbi.2013.40.issue-8>
- Menard, S. (2004). Six approaches to calculating standardized logistic regression coefficients. *The American Statistician*, 58, 218–223. <https://doi.org/10.1198/000313004X946>
- Mestre, F., Pita, R., Paupério, J., Martins, F. M. S., Alves, P. C., Mira, A., & Beja, P. (2015). Combining distribution modelling and non-invasive genetics to improve range shift forecasting. *Ecological Modelling*, 297, 171–179. <https://doi.org/10.1016/j.ecolmodel.2014.11.018>
- Mestre, F., Risk, B. B., Mira, A., Beja, P., & Pita, R. (2017). A metapopulation approach to predict species range shifts under different climate change and landscape connectivity scenarios. *Ecological Modelling*, 359, 406–414. <https://doi.org/10.1016/j.ecolmodel.2017.06.013>
- Millar, C. I., & Brubaker, L. B. (2006). Climate change and paleoecology: New contexts for restoration ecology. In M. Palmer, D. Falk, & J. Zedler (Eds.), *Restoration science* (pp. 315–340). Washington, DC: Island Press.
- Mysterud, A. (2006). The concept of overgrazing and its role in management of large herbivores. *Wildlife Biology*, 12, 129–141. [https://doi.org/10.2981/0909-6396\(2006\)12\[129:TCOOAI\]2.0.CO;2](https://doi.org/10.2981/0909-6396(2006)12[129:TCOOAI]2.0.CO;2)

- Phillips, S. J., Anderson, R. P., & Schapire, R. E. (2006). Maximum entropy modeling of species geographic distributions. *Ecological Modelling*, 190, 231–259. <https://doi.org/10.1016/j.ecolmodel.2005.03.026>
- Pita, R., Mira, A., & Beja, P. (2006). Conserving the Cabrera vole, *Microtus cabreræ*, in intensively used Mediterranean landscapes. *Agriculture, Ecosystems & Environment*, 115, 1–5. <https://doi.org/10.1016/j.agee.2005.12.002>
- Pita, R., Mira, A., & Beja, P. (2014). *Microtus cabreræ* (Rodentia: Cricetidae). *Mammalian Species*, 46, 40–70.
- QGIS Development Team. (2012). QGIS geographic information system. Open source geospatial foundation. <http://qgis.osgeo.org>.
- Quèzel, P., & Médail, R. (2003). *Écologie et biogéographie des forêts du bassin méditerranéen*. Paris (France): Elsevier.
- R Core Team. (2015). *R: A language and environment for statistical computing*. Vienna, Austria: R foundation for statistical computing. <http://www.R-project.org>
- Ramankutty, N., Evan, A.T., Monfreda, C., & Foley, J.A. (2010a). Global agricultural lands: Croplands, 2000. <http://sedac.ciesin.columbia.edu/data/set/aglands-croplands-2000>
- Ramankutty, N., Evan, A.T., Monfreda, C., & Foley, J.A. (2010b). Global agricultural lands: Pastures, 2000. <http://sedac.ciesin.columbia.edu/data/set/aglands-pastures-2000>
- Ridgeway, G. (2007). *Generalized boosted models: A guide to the gbm package*. <http://www.saedsayad.com/docs/gbm2>
- Rivas-Martínez, S. (1987). *Memoria del mapa de vegetación de España. Escala 1: 400000*. Madrid, Spain: ICONA.
- Rivas-Martínez, S. (2011). Mapa de series, geoseries y geopermaseries de vegetación de España. *Itinera Geobotánica*, 18, 5–424.
- Santos, S. M., Mathias, M. L., Mira, A., & Simões, M. P. (2007). Vegetation structure and composition of road verge and meadow sites colonized by Cabrera vole (*Microtus cabreræ* Thomas). *Polish Journal of Ecology*, 55, 481–493.
- Siebert, S., Henrich, V., Frenken, K., & Burke, J. (2013). Update of the digital global map of irrigation areas to version 5.171. <http://www.fao.org/nr/water/aquastat/irrigationmap/index.stm>
- Trabaud, L. (1993). From the cell to the atmosphere: An introduction to interactions between fire and vegetation. In L. Trabaud, & R. Prodon (Eds.), *Ecosystem research report 5: Fire in Mediterranean ecosystems* (pp. 13–21). Brussels, Belgium: European Commission.
- Vale-Gonçalves, H. M., & Cabral, J. A. (2014). New records on the distribution of three rodent species in NE Portugal from barn owl (*Tyto alba*) diet analysis. *Galemys*, 26, 100–104. <https://doi.org/10.7325/Galemys>
- Van Der Wal, J., Falconi, L., Januchowski, S., Shoo, L., & Storlie, C. (2014). *SDMTools: Species distribution modelling tools: Tools for processing data associated with species distribution modelling exercises*. <https://www.rforge.net/SDMTools/>
- Varela, S., Anderson, R. P., García-Valdés, R., & Fernández-González, F. (2014). Environmental filters reduce the effects of sampling bias and improve predictions of ecological niche models. *Ecography*, 37, 1084–1091.
- Varela, S., Lima-Ribeiro, M. S., & Terribile, L. C. (2015). A short guide to the climatic variables of the last glacial maximum for biogeographers. *PLoS ONE*, 10, e0129037. <https://doi.org/10.1371/journal.pone.0129037>
- Veloz, S. D., Williams, J. W., Blois, J. L., He, F., Otto-Bliesner, B., & Liu, Z. (2012). No-analog climates and shifting realized niches during the Late Quaternary: Implications for 21st-century predictions by species distribution models. *Global Change Biology*, 18, 1698–1713. <https://doi.org/10.1111/j.1365-2486.2011.02635.x>
- Weeks, A. R., Sgro, C. M., Young, A. G., Frankham, R., Mitchell, N. J., Miller, K. A., ... Hoffmann, A. A. (2011). Assessing the benefits and risks of translocations in changing environments: A genetic perspective. *Evolutionary Applications*, 4, 709–25. <https://doi.org/10.1111/j.1752-4571.2011.00192.x>
- Wildlife Conservation Society & Center for International Earth Science Information Network. (2005). Last of the wild project, version 2, 2005 (LWP-2): Global human influence index (HII) Dataset (Geographic). <http://sedac.ciesin.columbia.edu/data/set/wildareas-v2-last-of-the-wild-geographic>
- Willis, K. J., Araújo, M. B., Bennet, K. D., Figueroa-Rangel, B., Froyd, C. A., & Myers, N. (2007). How can a knowledge of the past help to conserve the future? Biodiversity conservation and the relevance of long-term ecological studies. *Philosophical Transactions of the Royal Society B*, 362, 175–186. <https://doi.org/10.1098/rstb.2006.1977>
- Zielhofer, C., Fletcher, W. J., Mischke, S., De Batist, M., Campbell, J. F. E., Joannin, S., ... Mikdad A. (2017). Atlantic forcing of Western Mediterranean winter rain minima during the last 12,000 years. *Quaternary Science Reviews*, 157, 29–51. <https://doi.org/10.1016/j.quascirev.2016.11.037>

BIOSKETCH

José Antonio Garrido-García is a mastozoologist specialized in rodents and bat conservation. He has conducted several studies of the interaction between man and mammal faunas in the Mediterranean Region during the Holocene based on palaeobiological projects in archaeological sites in Spain, France and Morocco.

Author contributions: J.A.G.G., R.C.S. and F.A.S. conceived the study; J.A.G.G. and R.C.S. collected the data; D.N.L. prepared the environmental data and analysed all the data; all authors analysed and discussed the results; J.A.G.G. and D.N.L. led writing of the manuscript.

SUPPORTING INFORMATION

Additional Supporting Information may be found online in the supporting information tab for this article.

How to cite this article: Garrido-García JA, Nieto-Lugilde D, Alba-Sánchez F, Soriguer RC. Agricultural intensification during the Late Holocene rather than climatic aridification drives the population dynamics and the current conservation status of *Microtus cabreræ*, an endangered Mediterranean rodent. *J Biogeogr.* 2018;45:448–460. <https://doi.org/10.1111/jbi.13134>